This Accepted Manuscript has not been copyedited and formatted. The final version may differ from this version.



Research Article: New Research | Sensory and Motor Systems

Robust and rapid air borne odor tracking without casting

Air borne odor tracking without casting

Urvashi Bhattacharyya¹ and Upinder Singh Bhalla¹

National Centre for Biological Sciences, TIFR, Bellary Road, Bangalore, Karnataka 560065, India

DOI: 10.1523/ENEURO.0102-15.2015

Received: 4 September 2015

Revised: 16 October 2015

Accepted: 19 October 2015

Published: 5 November 2015

Author Contributions: UB and USB Designed Research; UB Performed Experiments; UB and USB Analyzed data; UB and USB Wrote the Paper

Funding: NCBS/TIFR and DBT: BT/01/CEIB/09/111/03. UGC/ISF: F. No. 6-18 / 2014 (IC).

The authors declare no competing financial interests.

Funding: This work was supported by NCBS/TIFR and DBT, India, (BT/01/CEIB/09/111/03), UGC/ISF (F. No. 6-18 / 2014 (IC)). This work was supported by NCBS/TIFR and DBT, India, (BT/01/CEIB/09/111/03), UGC/ISF (F. No. 6-18 / 2014 (IC)).

Correspondence should be addressed to: Upinder Singh Bhalla, National Centre for Biological Sciences, TIFR, Bellary Road, Bangalore, Karnataka, India – 560065, (+91)- 80- 23666130. bhalla@ncbs.res.in

Cite as: eNeuro 2015; 10.1523/ENEURO.0102-15.2015

Alerts: Sign up at eneuro.org/alerts to receive customized email alerts when the fully formatted version of this article is published.

Accepted manuscripts are peer-reviewed but have not been through the copyediting, formatting, or proofreading process.

This is an open-access article distributed under the terms of the Creative Commons Attribution 4.0 International (http://creativecommons.org/licenses/by/4.0), which permits unrestricted use, distribution and reproduction in any medium provided that the original work is properly attributed.

eNeuro

http://eneuro.msubmit.net

eN-NWR-0102-15R1

Robust and rapid air borne odor tracking without casting

1		Title Page
2	1.	Manuscript Title: Robust and rapid air borne odor tracking without casting
3		
4	2.	Abbreviated Title: Air borne odor tracking without casting
5		
6	3.	List all Author Names and Affiliations in order as they would appear in the
7		published article
8		Urvashi Bhattacharyya ¹ & Upinder Singh Bhalla ¹
9		¹ National Centre for Biological Sciences, TIFR, Bellary Road, Bangalore, Karnataka,
10		India – 560065
11		
12	4.	Author Contributions: UB and USB Designed Research; UB Performed
13		Experiments; UB and USB Analyzed data; UB and USB Wrote the Paper
14		
15	5.	Correspondence should be addressed to: Upinder Singh Bhalla
16		(<u>bhalla@ncbs.res.in</u>); National Centre for Biological Sciences, TIFR, Bellary Road,
17		Bangalore, Karnataka, India – 560065, (+91)- 80- 23666130
18		
19	6.	Number of Figures: 17
20		
21	7.	Number of Tables: 0
22		
23	8.	Number of Multimedia: 4
24		
25	9.	Number of words for Abstract: 146

26		
27	10.	Number of words for Significance Statement: 103
28		
29	11.	Number of words for Introduction: 577
30		
31	12.	Number of words for Discussion: 1231
32		
33	13.	Acknowledgements: This work was supported by NCBS/TIFR and DBT, India,
34		(BT/01/CEIB/09/111/03), UGC/ISF (F. No. 6-18 / 2014 (IC)). We thank Raghav
35		Rajan, James P. Clement, Sonal Kedia and Adil G. Khan for comments on the
36		manuscript, Aditya Gilra and K Parthasarathy for help with design and analysis and
37		Sanjay Sane for discussions.
38		
39	14.	Conflict of Interest
40		No: The authors declare no competing financial interests
41		
42	15.	Funding sources: As mentioned in Acknowledgments.
43		
4.4		
44		

45 Robust and rapid air borne odor tracking without casting

47 Abstract

Casting behavior (zig-zagging across an odor stream) is common in air/liquid borne odor tracking in open fields; however terrestrial odor localization often involves path selection in a familiar environment. To study this we trained rats to run towards an odor source in a multichoice olfactory arena with near-laminar air-flow. We find that rather than casting, rats run directly towards an odor port, and if this is incorrect, they serially sample other sources. This behavior is consistent and accurate in the presence of perturbations such as novel odors, background odor, unilateral nostril stitching and turbulence. We developed a model that predicts that this run-and-scan tracking of air-borne odors is faster than casting provided there are a small number of targets at known locations. Thus the combination of best-guess target selection with fallback serial sampling provides a rapid and robust strategy for finding odor sources in familiar surroundings.

59 Significance Statement

Our study presents a novel olfactory task making it possible to study air-borne odor tracking
under well-controlled air-flow conditions, which elicit robust and spontaneous behavioral
patterns in rats. The study has numerous implications for the neuroethology of odor guided
target selection, and opens up interesting questions about how rats choose between strategies
under different conditions that they may encounter in the field. It further sets tight constraints
on olfactory sensory processing, both in terms of the sampling time, and in terms of decisionmaking. We speculate there may also be implications for how animals combine multisensory

input for odor guided navigation and target selection.

68

69

67

Introduction

70 Odor tracking is an essential capability for survival in many animals, and serves to find and 71 identify food, mates or predators. Many land animals can navigate towards the odor source using both air-borne and surface borne cues. 72 73 Studies show that dogs, humans, and rats zigzag across a surface odor trail during tracking, a 74 strategy known as casting (Gibbons, 1986; Porter et al., 2006; Khan et al., 2012). A similar zigzag strategy is also observed in insects (Vickers, 2000; Willis and Avondet, 2005; Lent et 75 al., 2013), fish (Montgomery et al., 1999; DeBose and Nevitt, 2008) and crustaceans 76 (Weissburg and Zimmer-Faust, 1994; Basil et al., 2000; Vickers, 2000) that have to use odor 77 information dispersed intermittently in fluid media. Apart from such zigzag tracking, animals 78 79 may also switch between different strategies to compensate for stimulus perturbations such as different odor gradients (Catania, 2006, 2013; Cardé and Willis, 2008; Reynolds et al., 2009; 80 Gomez-Marin et al., 2010, 2011). In turbulent conditions, vertebrates are known to display 81

82	phases of tracking that are different from each other in features such as speed, head
83	movement or odor sampling rate (Moore et al., 1991; Thesen et al., 1993). Rats also switch
84	rapidly between local and longer-range casting when they lose an odor trail (Khan et al.,
85	2012). Studies in ethologically relevant settings show wider plume sweeping trajectories of
86	animals with unilateral sensor blockage (Webster et al., 2001; Porter et al., 2006; Duistermars
87	et al., 2009; Khan et al., 2012; Catania, 2013). Similarly, animals shift in their orientation and
88	speed to adapt to the presence of masking or distracting background odors, where an animal
89	might have to discriminate between different potential stimuli (Party et al., 2013). They thus
90	learn to deploy a range of behaviors to compensate for perturbations, yet retain accurate odor
91	localization.
92	While stereo and casting strategies seem to be effective in many open field contexts, in many
93	cases there are additional cues. For example, in familiar environments there are likely to be a
94	few known paths leading to food sources, there may be visible targets or the animal may
95	remember the outcomes of past choices. Multisensory, and especially visual input, may also
96	help to change the olfactory task from 'where' to 'which'. For instance, in the context of
97	multiple choice elimination problems, the structure of the maze and spatial location of food is
98	important to determine strategy. These factors determine whether the animal eliminates
99	possible targets using a high divergence strategy (i.e. choosing locations as far as possible
100	from one trial to next, as in target number 1-4-2-3) or a lateral scanning strategy (going to the
101	nearest target from one just visited, as in target number 1-2-3-4,(Poucet et al., 1983; Buhot et
102	al., 1987). It is thus interesting to ask whether strategies other than zigzag 'casting' may be
103	suitable in air borne plume tracking, and how robust these may be to perturbations.
104	In this study, we developed a near-laminar-flow arena in which free-running rats could track
105	air-borne odors that were well-controlled with respect to location, background, and plume
106	dispersal. We find that rather than casting, rats proceed directly to a potential target with a

107	success rate that is much higher than chance, and scan serially across targets if this is wrong.
108	This behavior is robust to a range of conditions, such as odor changes, background odor,
109	unilateral nostril occlusion, and turbulence. We develop a model that shows that this behavior
110	is more efficient than casting for a wide range of conditions.
111	Materials and Methods
112	Animals: Five male Long Evan rats, 2-3 months old, were used for this study. All of the
113	experimental procedures were approved by the [Author University] institutional animal ethics
114	committee, in accordance with the guidelines of the [Author's] National Government and
115	equivalent guidelines of the <i>Society for Neuroscience</i> .
116	Thermocouple Implantation: To monitor respiration during the behavior task, rats were
117	implanted with thermocouple (PhysiTemp, Copper-Constantan, insulated) in their nasal
118	cavity (Figure 1a). Skull holes were drilled at ~ 5 mm anterior to the nasal suture and ~ 2 mm
119	lateral to the midline. The thermocouple wire was soldered onto a connector board which was
120	cemented using 6 skull screws. For all surgical procedures, rats were anaesthetized with
121	4% halothane and anaesthesia was maintained with $1% - 2.5%$ halothane. For the nostril
122	occlusion experiments, one of the nostrils was stitched shut with one or two stitches, while
123	the rat was under anaesthesia. The integrity of the stitches was checked after stitching and
124	before the training session. Removal of stitches was also done under anaesthesia. Post
125	surgical care involved cleaning the suture site with iodine solution, followed by application of
126	neomycin sulphate antibiotic powder over the wound. Rats were given the general analgesic
127	Dolo SUS (paracetamol, 100 mg/kg, Micro Laboratories) for 3 days and allowed to recover
128	for another 4 days before training was initiated.
129	Training box: The behavior arena was custom designed with a funnel shaped cross-section.
130	Its dimensions were 114.3 cm (1) x 88.9 cm (b) x 25.4 cm (h) with a curving angle of 44°

131	centred in the middle (Figure 1b). The broader opening of the funnel was divided into 7
132	compartments, each of dimension 12.7 cm (b) x 25.4 cm (h) and extending 15.24 cm (l) into
133	the box. The central 5 compartments were used to deliver odor. Rats were placed in the
134	narrow opening of the funnel (22.86 cm (l) x 15.24 cm (b) x 25.4 cm (h)) that served both as
135	the holding chamber and the reward delivery location between trials. Two circular exhaust
136	fans (11.43 cm diameter each) were fixed on the wall of the holding chamber to provide air
137	suction. All the experiments, except those requiring turbulent air flows, were conducted with
138	the broader end covered using an 'Activated Carbon Filter' (5 mm) sandwiched between fine
139	steel mesh.
140	Air flow velocity measurement: Anemometer measurements were conducted for the
141	running arena, starting from 6 cm ahead of the odor source compartments (Y=6) and ending 6
142	cm before the holding chamber (Y= 66 cm). The running arena was sampled in a grid of
143	dimensions 1 cm (X axis; range [-44:44] at maximum width) by 6 cm (Y axis; range [6:66]).
144	A hot wire anemometer (Kurz instruments 490-IS-M) was suspended in the closed behavior
145	box using magnets at each intersection of the grid points (Figure 1c). The tip of the
146	an emometer filament was positioned at $\sim 5~\text{cm}$ from the base. Data was collected using a
147	Measurement Computing data acquisition card (MCC DAQ PCI-6023) for 10 seconds at a
148	sample rate of 200/s. The anemometer voltage readings were calibrated against airflow
149	measured using the provided meter as well as against another pre-calibrated anemometer.
150	This curve was fitted using excel to the following equation:
151	velocity = 0.0817 *exp(12.795*V)
152	Where velocity is in m/s; and V = voltage out in volts. This conversion equation was used to

estimate the air flow rate from anemometer samples.

154	Smoke plume visualization: Smoke sticks were placed at the level of the odor source tube
155	for each compartment (~ 3 cm) and visualized using a planar laser-induced scattering
156	technique. The green laser pointer (< 5mW) was placed at the holding chamber. The light
157	passed through a cylindrical lens to form a sheet of \sim 2mm thickness (Figure 1d). Video was
158	captured using either a SONY Handycam DCR-SR300E (Movie 1, Movie 4) or iBall c12.0
159	webcam (Figure 13a, 13b). The images collected were stacked and contrast enhanced in
160	Image J for depicting the path of the smoke plume.
161	Odor stimulus delivery: A custom built air dilution olfactometer was used for odor delivery
162	(Figure 1e). Nitrogen at a constant flow rate of 0.05 l/m controlled using mass flow controller
163	(Alicat Scientific) was passed through a glass bead bubbler containing liquid odor. The
164	odorized nitrogen stream was diluted with 4.95 l/m of clean, humidified air to give a diluted
165	concentration of 1% odor (IAA, Cineole, Limonene tracking). Diluted odorized air stream at
166	1 l/m from a randomly selected odor port and 1 l/m of plain humidified air from the
167	remaining 4 ports was introduced into the behavior box using relay controlled solenoid
168	valves. Olfactometer design was changed for the background odor introduction experiments
169	(Figure 1f) to maintain the overall flow rate of the odor mix at 1 l/m. Tracking odor (1% at
170	0.5 l/m) was introduced along with the background odor (1% at 0.5 l/m) in the selected odor
171	port and clean humidified air (0.5 l/m) with background odor (1% at 0.5 l/m) was introduced
172	from the remaining four ports. The effective concentration of the odors in the stream was thus
173	reduced to half of that used in baseline experiments. The olfactometer and water delivery
174	were controlled using a custom written Microsoft Visual C# program. Odor source
175	compartment selection for each trial was randomly generated. Solenoids and their on/off state
176	visualizing light emitting diodes were controlled using a R16 relay board.

177	Olfact	cometer calibration and odor measurement in behavior box: The olfactometer was
178	calibra	ated using a Photo Ionization Detector (mini PID, Aurora Scientific). The probe was
179	sequer	ntially placed in-front of all the odor source outlets under both normal and background
180	odor c	onditions to verify odor concentration and delivery time. The PID map for odor in the
181	box w	as generated by placing the probe at $X = 1$ cm along the breadth and $Y = [0, 18, 30, 42,$
182	54, 66] cm along the length of the box, where $Y = 0$ marks the entrance of the odor
183	compa	rtments. We were only able to detect the presence and absence of odor at a given
184	positio	on using this technique. Calibration was done using isoamyl acetate as the tracking odor
185	with 4	repetitions of odor delivery in 2 sessions each at a given location.
186	Wirel	ess transmission: The thermocouple signals were obtained using a 15 channel wireless
187	transm	itter (Triangle Biosystems) transmitting signals at 100k samples/sec. Signals were
188	differe	entially digitized at 200 Hz and saved to disk using Measurement Computing DAQ
189	(PCI-6	6023) with custom written MATLAB (Simulink, MathWorks Inc.) program.
190	Train	ing procedure for navigation task: Implanted rats were trained to shuttle back and
191	forth between the odor port/compartment and the water reward/holding chamber. The training	
192	was established in four modules –	
193	(i)	Habituation to behavior box (2 days): Rats were placed in the behavior arena for 10
194		minutes each, for box exploration and habituation.
195	(ii)	Shuttle to water reward port (2 days): Rats were trained to shuttle back and forth
196		between the arena and the holding chamber for water reward, as well as initiation of
197		the next trial. Each session lasted for 10 minutes.
198	(iii)	Associate water reward with odor localization (~ 7 days): Odor was introduced in the
199		box at this stage. Rats were trained to identify the correct odor port and shuttle back to

200		receive water reward at the holding chamber. The rats were trained for 20 minutes
201		each session till they learned to self-initiate each trial.
202	(iv)	Achieve 80%: This was an extension to module (iii) where rats were required to
203		correctly locate the odor port and shuttle back to water reward with an accuracy of
204		80% or higher.
205	Expe	rimental tasks and their order
206	(i)	Tracking in Laminar air flow velocity: The basic training task was performed with
207		thermocouple implanted rats under laminar air flow conditions. 1 l/m of diluted odor
208		(IAA, 1%) was introduced from randomly selected odor port till rats learned to locate
209		the correct odor port with more than 80% accuracy. This training session lasted for
210		about 40 days.
211	(ii)	Task Generalization: In order to verify that the rat's response was not specific to IAA
212		cineole (1 l/m at 1%) and later limonene (1 l/m at 1%) were introduced as tracking
213		odors to confirm task repeatability and task generalization. The rats tracked cineole
214		and limonene for 6 and 4 days respectively.
215	(iii)	Tracking in the presence of novel background odor: Rats were assigned the task to
216		track one odor (limonene, 0.5%, 1 l/m) in the presence of an untrained (linalool,
217		menthone) odor as background conditions (0.5%, 1 l/m) flow. The protocol followed
218		was: (a) limonene + air (3 days) (b) limonene + linalool (2 days) (c) limonene + air (1
219		day) (d) limonene + menthone (2 days)
220	(iv)	Tracking under non stereo conditions: 4 rats were used for this task. Unilateral nostri
221		stitch was performed on either the left (2 rats) or the right nostril (2 rats) on the 3 rd
222		day of baseline tracking. Rats tracked odor with nostril stitch on the 4 th day, followed
223		by 2 days of recovery.

224	(v)	Tracking in the presence of familiar background odor: Same task as in (iii) except
225		with IAA as background odor. Protocol followed was (a) limonene + air (2 days) and
226		(b) limonene + IAA (5 days).
227	(vi)	Turbulent air flow conditions: The carbon filter mesh was removed for this task, such
228		that the air stream eddies could not be broken down into streamlined flow. Four rats
229		were assigned to track limonene (1% at 1 l/m flow rate) coming from a randomly
230		selected port.
231	Video	Imaging and Analysis: The behavior was recorded using a high speed camera
232	(Silico	on Imaging, SI-1920) and XCAP imaging software at 60 fps for 30 min long session per
233	rat ead	ch experimental day. 70000-120000 frames at an area of interest of 792 x 960 pixels
234	were o	captured per rat depending upon the duration of each session. Individual LEDs
235	corres	ponding to olfactometer switch, water reward, synchronization of thermocouple
236	record	ling and activation of each compartment source were also placed in the field of view.
237	Video	files were converted to .avi format and compressed using Virtual Dub for further
238	analys	sis. Wireless headstage had blue, green and red LEDs fixed on top for tracking. A
239	custor	n written MATLAB program identified the position of these LEDs for each frame using
240	a thres	shold for each color. Missing points were obtained using interpolation of the track using
241	cubic	spline method in MATLAB. Additionally, each frame was time stamped during
242	record	ling by the video acquisition software (EPIX-XCAP) for time synchronization with
243	therm	ocouple data. Further analysis with data from position coordinates was done in
244	MAT	LAB, Python and R.
245	Trial	outcome and strategy classification: For a given trial, the start and end points of the
246	trial w	vere respectively fixed at the frames where the rat emerged from, and returned to the
247	holdir	g chamber. Forward path was defined as the trajectory starting from the beginning of a

trial till first odor compartment entry, while return path of a rat was defined as the trajectory
from the last compartment exit till reaching the holding and reward chamber. Three main
criteria were used for a trial to be classified as direct (1) A single odor compartment entry in
the forward path (2) 85% of the forward track lay within a pre-defined region for a
compartmental source (Figure 1g) and a (3) relatively linear path with a maximum absolute
deviation from the projected odor path no greater than 22 cm (Figure 1h). For the purposes of
delivering enhanced reward for direct trials, an online analysis was done using only the first
of these criteria. The sub categorization of the direct trials into straight and offset was again
done on the basis of absolute maximum deviation from projected odor stream. Trials with
deviation up to 15 cm were termed as <i>straight</i> and those with deviation from 15 to 22 cm
were termed as offset. All paths having entries into multiple target compartments or large
lateral scans were clubbed under the serial strategy of target selection. For the outcome to be
classified as correct, the last compartment exit had to be from the odor source compartment.
Zig-zag trials were identified by visual inspection of forward tracks. From data based on
smoke plumes, an outline of ± 2.5 cm from the projected odor trail was taken as the maximum
width of the plume. We used a criterion of sharp changes in direction and at least two
crossings of the odor stream over a length of 80 cm from the holding chamber to the
beginning of the odor compartment to classify the behavior as 'casting'.
RMS deviation calculation: Figure 1h shows projected odor path for each compartment
used to calculate RMS deviation. These central odor lines were used to calculate the
deviation of rats' trajectory along X-axis. Subsequently, root mean square deviation for the
entire trajectory in the forward direction was calculated.
Sniffing frequency calculation: The radio-recorded thermocouple signal was first filtered
using a handness filter (MATI AB ellip with cutoffs $I.1 = 1. H1 = 0.5. I.2 = 20$ and $H2 = 30$

273

274

275

276

277

278

279

280

281

282

283

284

285

286

287

288

289

290

291

292

293

294

all values in Hz), and mean subtracted. It was then subjected to Fourier analysis using the numpy.fft.rfft function. As the original signal was noisy due to mechanical transients and transmitter noise, we applied the following criteria in order to select for acceptable recordings. We required that the frequency peaks obtained on the left and right channels were within 1.5 Hz of each other, and that the frequency was at least 3 Hz in the forward direction and 2 Hz in the return direction. We also required that the threshold for the forward-direction frequency peak height was > 0.007, and 0.009 for reverse. Finally, we required that the ratio of the second highest frequency peak to the highest peak was no more than 0.6. These criteria were developed based on visual inspection of > 100 trial waveforms, encoded in Python, and applied to all trials. Approximately 15% of trials cleared these criteria and were used for respiration analysis. **Sniff timing estimation:** We took the same filtered thermocouple signal as above. We first selected only waveforms where the signal had a standard deviation of greater than 0.015 V. We then required that the waveform should rise monotonically from -0.01 to above 0.01 V, and picked the zero-crossing point as the time of inhalation. Having done this for both left and right respiration channels, we combined the signals with the further requirement that if both channels reported a putative simultaneous inhalation it should be within 15 ms of each other. Finally, we eliminated cases where the time since last inhalation was less than 66 ms (corresponding to 15 Hz sniffing). These classification criteria were developed, as above, based on visual inspection of over 100 trial waveforms. The classification was encoded in Python and applied to all trials. Due to mechanical and transmission noise, only a small fraction of inhalation events cleared these criteria. These inhalation points were used to analyze sniff-triggered course changes.

Calculation of sniff-triggered course changes: To measure changes in orientation of rats
post sniff, the time-point of inhalation during forward track was marked as $\mathit{Frame}\ \theta$ (Time 0,
Figure 14). Displacement of rats along the X-axis (dx) per frame (dt) for the next 40 frames
(~680 ms) was calculated and averaged for all post sniff periods for a given session. As a
control, we computed the displacement as above, but triggered respectively from each of the
frames from sniff-4 to sniff+4. We averaged these displacement estimates to obtain control
displacements. At 60 frames per second, these 9 frames span approximately 133 ms which is
about the same as the average sniff duration. As mentioned above, the inhalation timing
measurements cleared criteria in only a fraction of recordings. Overall we were able to use 46
recording sessions which had sufficiently clean sniff timings.
Statistical Analysis: The non-normal distributions were tested for significance in MATLAB
using non-parametric test, Kruskal –Wallis (KW) ANOVA followed by Tukey HSD for
multiple comparisons (multcompare) at 5% significance values. These included speed, RMS
deviations and time taken for direct and serial tracking in each experimental module. Box
whisker plots in figure 4, 10, 11, 12, 13 represent the 25 th percentile (bottom edge) and 75 th
percentile (top edge) of the data. The median is represented by the gray line, most extreme
data points by whiskers and outliers marked individually with gray colored crosses. All error
bars in line graphs represent the SEM for Nd (number of direct trials) or Ns (number of serial
trials). Data for all rats were pooled to obtain the values of mean and sem across days (line
graphs) and for an entire block of experimental module (box whisker plots).
To compute if first entries for odor compartment were significantly different from a chance
flat distribution, we carried out chi- square test with the observed frequency of first entries
across diagonals (Figure 3) and expected frequency (total number of trials/25) for each rat
using MS Excel 'chitest'.

319	For side compartment preference calculation, Two tailed Student's t- test for each rat was
320	carried out in MATLAB between the number of first entries in off diagonal (k ± 1) non odor
321	compartments (8 bins) versus the remaining non odor compartments ($k \pm 2$, $k \pm 3$ and $k \pm 4$, 12
322	bins, Figure3).
323	Instantaneous speed and deviation for each forward track position till first entries were
324	pooled from all baseline days for all rats. Subsequently, the deviation and speeds were
325	averaged for every 1 cm increment from holding chamber till odor source. Paired sample <i>t</i> -
326	test was used to test for significance between averaged speeds in direct and serial tracks.
327	To test significant differences within post sniff displacement, and between post sniff vs.
328	control displacement, Z-test, followed by Bonferoni correction (0.05/46, α = 0.001) was
329	carried out for all sniff samples.
330	Model parameters: We estimated tScan in two ways. First we assumed that the rat
331	remembered which compartments it had tested, including the first entry. Thus the expectation
332	number of compartments to test in the case of a wrong entry was 2. Given that there was a 3
333	second difference between entry into the correct compartment for serial vs. direct trials
334	(Figure 4g), we obtained the estimated tScan = 1.5 sec. The second estimate of tScan came
335	simply from analyzing the videos where the rat sampled multiple compartments. We
336	manually analyzed 5-6 trials per rat totalling 55 entries in different compartments. We
337	obtained an estimate of 1.4 ± 0.07 seconds for tScan.
338	Results
339	Near-laminar air flow in behavior box: In order to monitor air-borne odor-guided behavior,
340	we designed a multi choice behavior arena similar to a closed air-tunnel with near laminar
341	airflow. Figure 1b shows a side view of the funnel shaped behavior box that includes a
342	holding chamber for the rat, a running arena and 5 different compartments as odor sources

344

345

346

347

348

349

350

351

352

353

354

355

356

357

358

359

360

361

362

363

364

365

366

(see methods). To measure air flow inside the box, we used a hot-wire anemometer suspended inside the box through the lid, using a pair of magnets, to minimize perturbations to the airflow (Figure 1c). The anemometer hung at 4-5 cm above the box floor, and was moved every 1cm along the breadth and 6 cm along the length of the box in order to sample flow (see methods). As measured by the anemometer, air flow in the behavior box was nearly laminar (~ 0.3 m/s air velocity, Figure 2a), with very low fluctuations of air velocity (Figure 2b) throughout the tracking arena. Expectedly, air velocity was slightly higher, with larger standard deviation in the region of the box which narrowed near the holding chamber. Maximum velocity was reached at the holding chamber area (~1 m/s), where exhaust fans pulled air out of the chamber. To visualize and measure odor plume dispersal under these conditions, we utilized 2 procedures. In the first procedure, smoke plumes were introduced at approximately the same position as the odor source, i.e. ~ 3 cm above the floor of the box. These plumes were visualized with a planar laser light sheet (Figure 1d). In the second procedure, we placed a photo-ionization detector (PID) at different positions in the box and used olfactometer stimulus delivery to check for presence or absence of odor at a given spot (see methods). Both these methods gave comparable results for trajectory and width of the odor stream. Using the videos, we ascertained that odor streams from different compartments were near-laminar and that plume structures were confined in a narrow (~4cm) band (Movie 1). Smoke plume videos and measurements of isoamyl acetate (IAA) presence obtained using the PID (Figure 2c) both showed distinct, non-overlapping odor streams from different compartment sources in the running arena. Some overlap was observed at the beginning of the holding chamber for adjacent compartments (C1 -C2, C2-C3, C3-C4 and C4-C5). Thus the airflow in the behavior arena was nearly laminar and narrow (~4 cm). The airflow was also found to be consistent upon repeated visualization using smoke plumes.

Rats advance directly to a target, and scan serially if it is wrong: All five rats learned to
identify the odor source accurately over the course of 18 days, as measured by the odorized
compartment being the last compartment visited before returning for the water reward (Figure
2d, see methods for trial outcome criteria). The accuracy after training was over 90%. Two
main trajectories of odor source location were observed: direct and serial (Figure 2e, 2f
Movie 2, Movie 3; recorded at 60 Hz, playback at 25 Hz). Automatic classification of these
paths was based on trajectories of the rat (see methods). As the direct path seemed to employ
odor tracking, we sought to obtain greater numbers of direct trials by giving the rats a 2-fold
higher water reward for direct trials. Despite this, each animal maintained a consistent,
relatively high rate of serial trajectories. To examine if casting behavior contributed to direct
tracking, we performed automatic offline classification of direct trials into two subcategories:
straight and offset (see methods). We found that overall, ~45% of trials were direct/straight,
\sim 7% were direct/offset, and \sim 48% were serial. The direct trials were examined visually for
typical features of casting behavior (see methods for criteria of selection). We found that only
8% of the total direct trials were classified as zig-zag.
Thus the first pass analysis of rat trajectories showed that even after extensive training they
persistently made a high fraction of errors in their choice of first compartment. The correct
trials were mostly in a direct line to the target, and zigzag casting behavior was infrequent.
Rats show a bias towards a subset of compartments but track odor well within this
subset.
We next sought to verify if direct runs were a result of a random selection of compartments
or guided by odor. Since the selectivity for direct trials was found to be independent of trial
number (Figure 2g), we ruled out motivation as a selection factor for direct vs. serial tracking.
Compartment bias was assessed by considering the distribution of first-entry into the five
compartments. If the choice was random, then the first entries should be equally distributed

392	among the 5 choices. Alternatively, if there were a preference towards a single compartment
393	this should show up in a strong bias of first-entry choices. The ability to track odors was
394	measured in two ways. First, we asked if the odorised compartment was the first visited.
395	Second, we asked if the most common errors were when the first entry was in the
396	compartment adjacent to the correct compartment.
397	In order to assess these factors we plotted a scatter grid of first compartments visited, against
398	odor compartment (Figure 3). From this dataset we extracted the distribution of odor
399	compartment activation (bottom histograms) and the distribution of first entries (left
400	histograms). We anticipated that rats might prefer to track the walls of the arena when doing
401	serial trials, and that they might do more direct trials at the beginning of the session when
402	they were more motivated. Instead we found that each rat had a characteristic preference for
403	three or four adjacent compartments (Figure 3, left histograms).
404	How accurate was rat tracking by odor? Assuming that rats do indeed prefer to go directly to
405	the odorised compartment, perfect tracking should yield points only along the diagonal. We
406	found that the scatter plot did have a higher density of points along the diagonal, but
407	compartment preferences were also clearly visible as horizontal bands (e.g., Figure 3b, 3c).
408	We confirmed that histograms of compartment preference were significantly different from a
409	flat distribution (chi-square test, $p \le 10^{-81}$ all rats). We also estimated the fraction of correct
410	trials with direct tracking, averaged over all compartments as a function of time (Figure 4a).
411	If compartment entries were independent of odor, one would expect this fraction to be 0.2 (as
412	there were 5 compartments). Instead the fraction varied between 0.4 to 0.6. Another
413	qualitative trend was that the flanks of the diagonal were also over-represented (Figure 3, right
414	column histograms, off diagonal $k{\pm}1),$ suggesting that when rats made an error, it was
415	mostly to adjacent compartments. We found that the off-diagonal flank visits ($k \pm 1.8$ bins)

416	were weakly significant in 3 rats over visits in the remaining non odor compartments ($k \pm 2$, $k \pm 2$)
417	± 3 and k ± 4 , 12 bins, p = [0.026, 0.019, 0.036], Two-Tailed Student's <i>t</i> - test).
418	Of all the serial trials, 43% were correct upon second entry; 31% were correct when the first
419	entry was adjacent and $\sim 11\%$ were correct when first entries were not adjacent to the correct
420	compartment. Notwithstanding these general trends, it was clear that each rat showed
421	idiosyncratic preferences for a subset of compartments, mostly centred around the middle
422	compartment. In trials where odor was delivered to these compartments the odor guided
423	tracking was significantly higher than chance.
424	Rats run slower but sniff faster during tracking.
425	We next tested if first-compartment targeting errors were due to reduced monitoring of the
426	odor environment. To do this we asked if rats ran and sampled differently when tracking,
427	compared to returning to the reward chamber. We also compared running speed and sampling
428	between direct and serial trajectories.
429	We observed that rats ran significantly slower (Figure 4c) in the forward direction as
430	compared to the return direction (data shown for correct trials: forward direct, $FD = 76.23$
431	± 0.4 cm/s, return direct, RD = 109.6 ± 0.3 cm/s, forward serial, FS = 69.4 ± 0.3 cm/s and
432	return serial, RS = 108.2 ± 0.3 cm/s). The forward speeds for direct and serial trials were
433	significantly different from each other as well (Figure 4d, p =0, Kruskal Wallis Tukey HSD
434	test).
435	Serial tracking was clearly less efficient than direct (Figure 4b-h, Figure 16a), and had some
436	attributes of exploration. It differed from the direct trials in features such as speed, deviation
437	from odor path and total time to finish trial. The instantaneous deviation of the trajectory
438	from the odor path in direct and serial trials is shown in Figure 5 (panels a-e). Left column
439	shows the deviation values for direct trials, while the central and right column shows the
440	naths overlaid on observed plume trajectories using PID. The root mean square (RMS)

deviation of each rat's trajectory from the odor path was between 4 to 6 cm (all rats pooled
mean = 5.5 cm, ± 0.07 cm, Nd = 1851) for direct trials and between 15 to 20 cm (all rats
pooled mean = 18.6 cm, ± 0.18 , Ns = 2150) for serial trials (Figure 4e). Pooled across all
days for all the rats, the averaged RMS values in forward and return paths for both the direct
and serial trials were significantly different from each other ($p = 0$, KW – Tukey HSD test,
Figure 4f). Direct trials were also shorter in duration (p \leq 10^{-10} , KW-Tukey HSD test) with a
mean time of $\sim 4.8 \pm 0.03$ sec across all rats (Figure 4g, 4h). In contrast, rats took much
longer time to finish serial trials ($\sim 7.4 \text{ sec} \pm 0.09 \text{ sec}$).
All five rats were implanted with thermocouples to measure respiration frequency during
tracking. As shown in Figure 6a, rats sniff faster while running towards the odor source
(forward sniff rate, 8-10 Hz) as compared to running towards the water reward (return sniff
rate, 5-7 Hz). This elevated sampling behavior was observed irrespective of whether the rats
were running directly or serially towards the target (Figure 6b). We next asked if high
sniffing rates was related to the running speed of the rat. Figures 7 and 8 show instantaneous
speeds of the animals during direct and serial tracking respectively for a single day. Left
column shows forward speeds and right column shows the return speeds for all 5 rats (panel
a-e). Large variations in the instantaneous speeds between rats were observed for forward
tracking as well as between direct and serial trajectories. For example, in some direct tracks,
rats were slow at the holding chamber, sped up in the middle of the arena, and then slowed
down as they approached the odor source. In other direct tracks, rats had near constant (low
or high) speeds throughout the run. On the other hand, instantaneous speeds during the return
run to water reward was similar in all animals and in both the strategies. Strikingly, in all
cases the sampling frequency was higher during the forward run even though the average
running speed was lower (Figure 6c). In summary, rapid respiration was associated with the
tracking phase of each trial, rather than exertion due to faster running. There was a small

466	difference in running speeds between direct and serial tracking, but the return run was always
167	significantly faster.
468	Direct and serial trials differ due to early decision making.
469	Since in our setup plumes converge near the holding chamber (~ 80 cm, Figure 1h, 2c), errors
470	in route selection are possible if rats select targets using plume information near the holding
171	chamber and move upwind. Such behavior has been observed in <i>Drosophila</i> (Breugel and
172	Dickinson, 2014) where flies use early cues to surge upwind, followed by a later casting
173	phase upon loss of contact with odor.
174	We first asked if there was a difference between serial and direct trials that ended in the same
175	compartment. We reasoned that if the movement was odor guided in direct but not serial
476	trials, then the trajectories should differ. We found that overall trajectories to the same
177	compartment could be either non-overlapping (example one day session, Figure 9 a-c) or
478	overlapping (Figure 9 d-f) indicating that target routes are not necessarily fixed. A similar
179	variability was seen in the initial (above 80cm) part of the track, which was highly
480	overlapping in some cases but different in others (Figure 9a-f).
481	We then checked if errors leading to serial trials were evident at the outset of the track. We
182	computed the distance from the rat track to the odor plume in direct and serial trials
183	respectively (see methods). On average rats already showed approx. 2 cm greater deviation in
184	serial trials even very close to the holding chamber (Figure 9g). Except for rat B (Figure 9h,
185	top panel), all other rats start out further from the odor plume in serial trials (Figure 9h).
186	As a final comparison of direct and serial trajectories, we compared the instantaneous speed
187	profile for direct and serial trials. We found that the average instantaneous speed profile (see
188	methods) diverged slightly between serial and direct trials after ~70 cm along the length of
489	the box (Figure 9i, p<0.01, paired t -test). Overall, these comparisons suggest that serial and
103	the box (1 1gare 71, p 30.01, panet 1-10.51). O veran, these companisons suggest that serial and

490 direct trials are different near the holding chamber and diverge further as they approach the 491 selected compartment. 492 Rats can generalize odor tracking to novel odors: At this stage we had characterized the 493 basic air-borne odor-guided tracking behavior of the rat in a known arena. In the next set of experiments we examined a range of perturbations to assess the robustness of the behavior. 494 We first asked if the rats could track odors other than the one they were trained on. When 495 presented with novel odor (Cineole) for the first time, tracking accuracy initially dropped, 496 followed by a recovery period over 4 days (Figure 10a). A second novel odor presentation 497 498 (Limonene) took a much shorter time (1 day, Figure 10a) to locate. Both direct and serial tracking accuracies were affected with a larger effect on serial tracking (Figure 10b, 10c). 499 500 The fraction of trials where animals took a direct path varied between the 5 rats (Figure 10d), 501 though in the case of cineole, the fraction of direct trials decreased in each module, followed 502 by an increase as the learning progressed. To observe the effect of different conditions on tracking, we focused on RMS, speed and time for direct trials. The dependence of these 503 parameters on training is shown in Figure 10e, 10g and 10i respectively. There was a small 504 505 but significant increase in RMS values when data were pooled for all days of a given module, (Figure 10f, **p < 10^{-10} , KW- Tukey HSD test) with introduction of cineole (6.01 ± 0.1 cm, 506 Nd = 921) and limonene (5.9 ± 0.1 cm, Nd = 724). The distributions of speeds across days for 507 cineole and limonene were significantly different than baseline (Figure 10g, p $< 10^{-5}$ KW -508 Tukey HSD test), while the average speed pooled across all days was lower for cineole (77.5 509 \pm 0.6 cm/s for cineole versus 80.6 ± 0.66 cm/s for limonene, Figure 10h, **p < 10^{-10} , KW-510 Tukey HSD test). Decrease in total trial time for direct trials was small but significant ($4.5 \pm$ 511 0.05 sec for cineole and 4.3 ± 0.05 sec for limonene, **p < 10^{-25} , KW-Tukey HSD test, 512 Figure 10i, 10j) as compared to the baseline trials. Thus rats were able to learn and generalize 513 the odor tracking task to different odors, over a few days. Although there were changes in 514

515	RMS deviation from the odor track, and also in the speed of the direct trials, these were quite
516	small.
517	Unilateral nostril occlusion has varying effects on trial time, but not on accuracy: Rats
518	use bilateral stereo input to achieve higher accuracy in odor source localization as well as
519	surface-borne odor tracking (Porter et al., 2006; Rajan et al., 2006; Khan et al., 2012; Catania,
520	2013). We tested rats with unilateral nostril block in our air-borne odor source localization
521	task with Limonene as the tracking odor. Remarkably, we observed no differences in
522	accuracies (Figure 11a, 11b) or averaged direct trial RMS deviation (Figure 11d) pooled
523	across all rats. Barring one rat (Figure 11c), the fraction of direct trials was also consistent
524	across days. Small differences were observed in speeds and trial times of rats on the day of
525	the nostril stitch. There was a significant increase (** $p < 10^{-10}$, KW – Tukey HSD, Figure
526	11e, 11f) in the time taken to finish direct trials during stitch days (Nd = 91, mean = $6.17 \pm$
527	0.17 sec) as compared to pre (Nd = 425, mean = 4.89 ± 0.08 sec) and post (Nd = 243, mean =
528	5.12 ± 0.1 sec) stitch days. Similarly, forward speeds for direct trials were also slower (**p <
529	10^{-7} , KW – Tukey HSD test, Figure 11g, 11h) during the stitch days (69.2.3 \pm 1.9 cm/s
530	compared to $\sim\!80$ cm/s for both pre and post stitch days). Thus, animals maintained high
531	accuracy in tracking despite loss of stereo information, at the expense of small increases in
532	trial time and decreased forward speeds.
533	Identity of background odor determines tracking accuracy: In natural environments,
534	animals have to locate odor direction in the context of many different background odors. To
535	test the effect of odor background on tracking, we introduced background odors into all of the
536	five compartments. To keep the total odor concentration in the system at 1%, our tracking
537	odors were at 0.5% saturation at 0.5 l/min, and so was the background odor (see methods).
538	On separate days we introduced background odors linalool, and menthone (unfamiliar odors)
539	and isoamylacetate (IAA, familiar odor). In all these cases the animals were tasked to locate

540	limonene coming from a single compartment. We started these experiments with the tracking
541	odor (limonene at 0.5% saturation) in an air background. This reduced concentration led to an
542	initial changed baseline for multiple behavioral parameters, including accuracy and fraction
543	of direct trials. These rapidly returned to baseline (Figure 12). We observed that different
544	background odors had different effects on tracking accuracy, but the animals soon recovered.
545	For example, the presence of background linalool (a terpene alcohol) had no visible effect on
546	any of the parameters like total, direct and serial accuracy (Figure 12a, 12c and 12d, grey
547	shaded region). Background menthone (which belongs to the same family of cyclic terpenes
548	as the tracking odor limonene) had a modest effect on total, direct and serial accuracies
549	(Figure 12a, 12c and 12d, red shaded region).
550	In a separate block of sessions we again introduced limonene at 0.5% in an air background,
551	followed by background IAA, which had previously been used as a reward odor. IAA had a
552	strong effect (Figure 12a, 12c, 12d, green shaded region). Our interpretation is that rats
553	identified IAA coming from each compartment as a potential reward odor. They thus were
554	not able to discriminate between odor targets, initially reducing their tracking accuracies to
555	chance (20%). This outcome serves as an additional control to show that rats were indeed
556	relying on odor to carry out their compartment selection.
557	The effects of background on other measures of performance were small or absent. Fraction
558	direct was unchanged in all but one rat (Figure 12b). RMS deviation from new baseline (6.9 \pm
559	0.14 cm, Nd = 524) for direct trials decreased only with linalool (mean = 6.0 ± 0.18 cm, Nd =
560	295, Figure 12e, 12f, ** $p < 10^{-3}$, KW – Tukey HSD test) as background, but not menthone
561	(mean = 6.4 ± 0.2 cm, Nd = 241). No differences were observed with pooled IAA
562	background (mean = 6.4 ± 0.1 , Nd = 540) as well. We observed decreased speed (Figure 12g,
563	12h) and increased time (Figure 12i, 12j) with linalool (75 \pm 1.1 cm/s) and menthone (77 \pm
564	1.2 cm/s) compared to new baseline (82.7 \pm 0.8 cm/s, with **p < 10 ⁻⁸ , using KW - Tukey

565	HSD test). Again, no such differences were observed with IAA as background (83.1 \pm 0.8
566	cm/s). In summary, background odors did have an initial impact on rat tracking behavior but
567	with learning rats were able to discriminate between the background and foreground, and
568	accurately track the relevant odor.
569	Increased turbulence was ineffective in changing tracking behavior:
570	Natural odor environments are highly variable and frequently turbulent. Studies on effect of
571	increased turbulence have shown reduction in tracking accuracy in blue crabs (Keller and
572	Weissburg, 2004), but no change or an increase in the tracking accuracy of whelks (Ferner
573	and Weissburg, 2005) and crayfish (Kozlowski et al., 2003; Moore et al., 2015). To study the
574	effect of dispersed odor plumes on tracking, we removed the carbon filter near the
575	compartment end, without changing the rate at which the air was suctioned into the box. This
576	resulted in introduction of eddies into the air stream and a broader odor plume (Movie 4,
577	Figure 13a). As the turbulent plume progressed, its width exceeded the width of the
578	compartment and its profile was highly variable in both temporal and spatial dimensions. In
579	our experiment, with the exception of one rat (Rat A), we did not observe any change in
580	accuracy (Figure 13c-d) or fraction direct trials (Figure 13e). On the other hand, RMS
581	deviation increased (Figure 13f, 13g from 6.4 ± 0.16 cm, Nd = 325, to 7.2 ± 0.14 cm cm, Nd
582	= 522, ** p < 10^{-3}). The effect on speed and total time of tracking were small but significant
583	(mean speed = 82 ± 0.7 cm/s, Figure 13h, 13i, **p < 10^{-14} ; mean time = 3.9 ± 0.7 sec, Figure
584	13j, 13k, ** $p = 10^{-3}$, KW-Tukey HSD test). We looked into the sub-categories of direct
585	tracking, and found an increase of offset trials from 6 to 11 %. No increase in the fraction of
586	trials with casting was observed (8%). In effect most rats were readily able to compensate for
587	turbulence in their odor tracking performance with few modifications to their tracking
588	behavior.
589	Sniff-triggered course corrections were not observed.

590	We analyzed if sniffs triggered changes in trajectory during tracking	ng under any of these
591	conditions. To do this we computed sniff-triggered trajectory histo	grams and compared these
592	against non-sniff-triggered trajectories (methods). We did not find	significant differences
593	between the sniff-triggered and control cases in any of the 46 out of	of 350 recording sessions
594	that cleared sniff-classification criteria (criteria specified in method	ds; data shown till 192 ms
595	post sniff, Figure 14, a-d).	
596	In 5 cases (pre nostril baseline and IAA background), there were a	pparent deviations at the 8
597	10 th frame (i.e. 137-170 ms post inhalation, Figure 14, c-d), but the	ese were not significantly
598	different from the control. If trajectory corrections were sniff related	ed, they would be expected
599	to happen at around this time (Wesson et al., 2008). Thus the curre	ent sniff and tracking data
600	do not support the hypothesis of sniff-triggered changes in tracking	g trajectories.
601	Run-and-scan is more efficient than casting over a wide range	of conditions
602	To integrate these observations, we constructed two models to bett	ter understand the trade-
603	offs between run-and-scan behavior and the familiar casting strate	gy. In the first model, we
604	used the observations that rats used direct trials about 50% of the t	ime (Figure 4a) and were
605	correct almost all the time in such cases (Figure 16a). We also use	d the observation that error
606	trials adjacent to the correct port accounted for about 25% of the to	otal trials (Figure 3). We
607	assumed that in such cases the rats immediately corrected themselves	ves, thus wasting only one
608	scan time (tScan). In the remaining 25% of cases, we assumed that	t the rats never re-sampled
609	an already visited compartment, and took precisely tScan seconds	to visit each. Thus the
610	expected time for a trial was:	
611	tRun = D/vRun + tScan * (0.25 + 0.25 * (N-1)/2) which simplify	ies to
612	tRun = D/vRun + tScan * (N+1)/8	Eq (1)

613	Here tRun is expectation time to complete the run, D, is distance to target(s), vRun is runn	ning
614	speed, and N is number of compartments.	
615	In the second version of this model, the rats still used direct trials 50% of the time. Here v	ve
616	assumed that if the rats made an error, they serially scanned the remaining compartments	
617	including the adjacent ones. We tested this model because only 3 of our 5 rats showed a	
618	significantly higher likelihood than chance of picking a compartment adjacent to the corre	ect
619	one (Figure 3). We again assumed that the rats never re-sampled and took the same tScan	
620	seconds per compartment. We then obtained:	
621	tRun = D/vRun + tScan * (N-1)/4 Eq (2)	
622	Finally, we assumed that in casting behavior the animals advanced toward the target at at	t
623	fixed speed vCast, thus giving the model	
624	tCasting = D/vCast Eq. (3)	
625	In these models, N=5 and D~1m are known from the configuration of the arena. The runn	ning
626	speeds vRun for both run and scan were about 0.8 m/s (Figure 4d). While we are not awar	re o
627	direct data for running speeds of rats during free-running casting behavior (vCast), previous	ous
628	studies on surface borne odors suggest that casting may become limited by sniffing rates a	at
629	around 0.2 metres/s (Khan et al., 2012). Here we assumed that the speed during casting w	as
630	roughly vCast = 0.3 m/s, though the broad conclusions of the model were not very sensiti	ve
631	to this. We estimated tScan as 1.5 seconds, as described in the methods. We computed run	n-
632	times for a range of N and D for each strategy and plotted their difference (Figure 15). The	nis
633	gave the surprising prediction that run-and-scan was a better strategy in most cases,	
634	especially at greater distances. In summary, this model suggests that the run-and-scan	

strategy is preferable at greater distances in situations where there are known targets, but casting was advantageous for free-range search.

We have found that rats achieve high accuracy and robust performance in tracking air-borne

Discussion

637

638

639

640

641

642

643

644

645

646

647

648

649

650

651

652

653

654

655

656

657

658

odors in a familiar environment, but do not utilize casting (zig-zag scanning) to do this. Instead they preferentially attempt a subset of targets and approach them in a rapid, odorguided but somewhat error-prone manner. They resort to serial scanning if their initial target selection is incorrect. We suggest that this "run-and-scan" behavior is an alternate to casting in an environment where there are a small number of known targets or potential routes, and may offer advantages in speed and robustness. Casting is a well-established odor-tracking strategy, and has been observed in numerous surface-borne as well as air/water borne contexts (Vickers, 2000; Porter et al., 2006; Khan et al., 2012). A distinct strategy has been reported for short-range target selection: casting to ascertain gradients, followed by stereo to home in on the target (Catania, 2013). Our results show that, in our specific arena, animals achieve good odor-guided performance but do not rely on casting. Surprisingly, our model suggests that the familiar casting strategy is not as efficient as run-and-scan in most long-range contexts where there is additional target distance information. If we strip away the model terms related to direct trials, run-and-scan wins simply because the initial run saves time, and subsequent scanning is not very expensive as long as there are not too many possible targets or they are not too far apart. Casting becomes essential when the distance to the odor source is unknown. Extrapolating from the conditions of our arena, we suggest that the key determinants for observing natural run-and-scan behavior would be a) known distances or paths to the targets, either through previous experience or through other sensory cues, b) a few distinct targets rather than a continuum,

660

661

662

663

664

665

666

667

668

669

670

671

672

673

674

675

676

677

678

679

680

681

682

and c) upwind odor cues. While we are not aware of studies that have examined this, we suggest that these conditions may occur frequently in natural contexts. The behavior we observed was quite robust to perturbations. While the behavioral protocol almost ensured high final target-selection accuracy, our emphasis here was on the choice between direct and serial trials, and the quantitative readouts of tracking during the trials. To first order, it was remarkable how consistent the basic run-and-scan behavior was under a wide range of manipulations. The only exception to this general observation of robustness came when we used a familiar odor (IAA) as background along with the tracking odor. In this case the animals were simply confused about the identity of the odor that specified reward, and in a few days learned the task in this context as well. When the quantitative parameters of behavior were examined, it was clear that the rats did not randomly pick a target and then ignore odors as they ran: the animals were sampling rapidly for the entire route, and their speed was slower than when they were running back for the reward. In some cases a last-second course correction was apparent (Figure 5d- 5e, left and central column). However, unlike in casting behavior, we did not see evidence for snifftriggered course corrections (Figure 14). Further, in difficult situations (unilateral nostril block, background odor, or turbulence) there was a small but significant effect on speed. On average, rats correctly made a direct entry into the odorized compartment 40-70% of the time (Figure 16b – 16f). This fraction varied within this range across compartments and with perturbations. We interpret this to mean that the animals did indeed improve performance and fraction of successful direct trials by continual monitoring, and sustained above-chance direct trials despite perturbations. How efficient is stereo guidance in these conditions? Previous results for air-borne as well as

surface borne odor tracking show a characteristic scanning or casting behavior (Thesen et al.,

683	1993; Vickers, 2000; Porter et al., 2006; Gomez-Marin et al., 2011; Khan et al., 2012). This
684	has been shown to be quite sensitive to stereo sampling (Duistermars et al., 2009; Gomez-
685	Marin et al., 2010; Khan et al., 2012; Catania, 2013). However, target selection has been
686	shown to have multiple phases (Moore et al., 1991; Thesen et al., 1993), including an initial
687	non-stereo-guided phase and subsequent refinement using stereo (Catania, 2013). Here we
688	found that stereo has little effect on odor source localization for air-borne odors coming from
689	known potential targets. Our results for nostril occlusion are in contrast to surface borne
690	tracking in animals (Porter et al., 2006; Khan et al., 2012) where increased deviations are
691	observed with unilateral sensor block. One explanation is that in our behavioral setup, air
692	borne cues are distant in nature, whereas use of bilateral comparison is more effective near
693	the source of the odor, where concentration gradients are steepest (Catania, 2013).
694	Why do rats persist with serial scanning? In our study, the rats adopted the direct trajectory
695	only 40-70% of the time, even though the direct trials took less time and were as accurate as
696	serially completed trials. Further, additional reinforcement (2x reward) for direct trials did not
697	raise the fraction of direct trials to over 70%.
698	One possible explanation for the persistence of serial trials could be the preference of rats for
699	the side chambers as rats are known to prefer to move along walls. In contradiction to this
700	hypothesis, we found that the first compartment entry in direct as well as serial trials was in
701	fact biased towards the central compartments (Figure 3, Figure 17).
702	Another possibility might be the dichotomy between goal-directed and habitual behavior
703	(Balleine and O'Doherty, 2010; Keramati et al., 2011). In our work the direct tracking could
704	be interpreted as goal-directed as it is based on immediate assessment and decision-making
705	based on sensory data, and the serial as a habitual tracking where actions could be initiated
706	without deciding on where the target is. However, both serial and direct trials had high

707	sniffing rates, and rats were actually running slower in the serial trials. Thus it is unlikely tha
708	one could classify serial trials as other than goal-directed.
709	From our observation that serial and direct trials differ very early in the track, we suggest that
710	initial trajectory decisions are made early but in an error-prone manner (Figure 9). Thus seria
711	tracks result from an incorrect guess, whereas in direct trials the early guess remains on the
712	odor trail. Thus, near-guesses may account for the high incidence (~46%) of serial trials
713	where the first entry was in the compartment adjacent to the correct one. How might the run-
714	and scan behaviour apply in ethological contexts? In one scenario, there may be a small
715	number of traversable tracks leading from the entrance of a burrow to possible food (and
716	odor) targets. When tracking, the animal would run towards its best guess and should it fail
717	would scan through the others. Another manifestation of the scan phase of this behavior may
718	occur when animals forage in a target-rich environment such as a refuse dump, rapidly
719	sampling one location after another.
720	We suggest that serial scanning is frequent simply because rats prioritize speed over accuracy
721	in this behavior. Indeed, from the model calculations, the higher-than-chance accuracy of
722	direct trials could be viewed as a small bonus, but not the central advantage of the run-and-
723	scan strategy. Thus serial scanning should be seen not as inefficient fallback behavior, but
724	rather as the key part of the run-and-scan behavior pattern that is effective at long distances
725	and when the possible targets are known.
726	References
727	Balleine BW, O'Doherty JP (2010) Human and rodent homologies in action control:
728	corticostriatal determinants of goal-directed and habitual action. Neuropsychopharmacology
720	35:48 60

- 730 Basil JA, Hanlon RT, Sheikh SI, Atema J (2000) Three-dimensional odor tracking by
- 731 Nautilus pompilius. Journal of Experimental Biology 203:1409–1414.
- 732 Breugel F van, Dickinson M. (2014) Plume-Tracking Behavior of Flying Drosophila
- 733 Emerges from a Set of Distinct Sensory-Motor Reflexes. Current Biology 24:274–286.
- Buhot MC, Poucet H (1987) Role of the Spatial Structure in Multiple Choice Problem-
- 735 Solving in Golden Hamsters. In: Cognitive Processes and Spatial Orientation in Animal and
- 736 Man. In (Paul Ellen CT-B, ed), pp124–134. Springer Netherlands.
- 737 Cardé RT, Willis MA (2008) Navigational strategies used by insects to find distant, wind-
- borne sources of odor. Journal of chemical ecology 34:854–866.
- 739 Catania KC (2006) Olfaction: underwater'sniffing'by semi-aquatic mammals. Nature
- 740 444:1024-1025.
- 741 Catania KC (2013) Stereo and serial sniffing guide navigation to an odour source in a
- mammal. Nature communications 4:1441.
- 743 DeBose JL, Nevitt GA (2008) The use of odors at different spatial scales: comparing birds
- with fish. Journal of chemical ecology 34:867–881.
- 745 Duistermars BJ, Chow DM, Frye MA (2009) Flies require bilateral sensory input to track
- odor gradients in flight. Current Biology 19:1301–1307.
- 747 Ferner MC, Weissburg MJ (2005) Slow-moving predatory gastropods track prey odors in fast
- and turbulent flow. Journal of Experimental Biology 208:809–819.
- 749 Gibbons B (1986) The intimate sense of smell. Natl Geographic Mag 170:324–361.

- Gomez-Marin A, Duistermars BJ, Frye MA, Louis M (2010) Mechanisms of odor-tracking:
 multiple sensors for enhanced perception and behavior. Frontiers in cellular neuroscience 4.
- 752 Gomez-Marin A, Stephens GJ, Louis M (2011) Active sampling and decision making in
- 753 Drosophila chemotaxis. Nature communications 2:441.
- Keller TA, Weissburg MJ (2004) Effects of odor flux and pulse rate on chemosensory
- 755 tracking in turbulent odor plumes by the blue crab, Callinectes sapidus. The Biological
- 756 Bulletin 207:44-55.
- 757 Keramati M, Dezfouli A, Piray P (2011) Speed/accuracy trade-off between the habitual and
- 758 the goal-directed processes. PLoS computational biology 7:e1002055.
- 759 Khan AG, Sarangi M, Bhalla US (2012) Rats track odour trails accurately using a multi-
- layered strategy with near-optimal sampling. Nature communications 3:703.
- 761 Kozlowski C, Voigt R, Moore PA (2003) Changes in odour intermittency influence the
- 762 success and search behaviour during orientation in the crayfish (Orconectes rusticus). Marine
- and Freshwater Behaviour and Physiology 36:97–110.
- 764 Lent DD, Graham P, Collett TS (2013) Phase-dependent visual control of the zigzag paths of
- navigating wood ants. Current Biology 23:2393–2399.
- 766 Montgomery JC, Carol JD, Matthew D, Halstead B. D(1999) Olfactory search tracks in the
- Antarctic fish Trematomus bernacchii. Polar Biology 21:151–154.
- 768 Moore PA, Scholz N, Atema J, (1991) Chemical orientation of lobsters, homarus americanus,
- in turbulent odor plumes. Journal of Chemical Ecology 17:1293–1307.

- 770 Moore PA, Ferrante PA, Bergner JL (2015) Chemical Orientation Strategies of the Crayfish
- are Influenced by the Hydrodynamics of their Native Environment. The American Midland
- 772 Naturalist 173:17–29.
- 773 Party V, Hanot C, Büsser DS, Rochat D, Renou M (2013) Changes in odor background affect
- the locomotory response to pheromone in moths. PloS one 8:e52897.
- Porter J, Craven B, Khan RM, Chang S-J, Kang I, Judkewitz B, Volpe J, Settles G, Sobel N
- 776 (2006) Mechanisms of scent-tracking in humans. Nature neuroscience 10:27–29.
- Poucet B, Buhot-Averseng M-C, Thinus-Blanc C (1983) Food-searching behavior of cats in a
- multiple-choice elimination problem. Learning and motivation 14:140–153.
- Rajan R, Clement JP, Bhalla US (2006) Rats smell in stereo. Science 311:666-670.
- 780 Reynolds AM, Swain JL, Smith AD, Martin AP, Osborne JL (2009) Honeybees use a Lévy
- 781 flight search strategy and odour-mediated anemotaxis to relocate food sources. Behavioral
- 782 Ecology and Sociobiology 64:115–123.
- 783 Thesen A, Steen JB, Doving K (1993) Behaviour of dogs during olfactory tracking. Journal
- of Experimental Biology 180:247–251.
- 785 Vickers NJ (2000) Mechanisms of animal navigation in odor plumes. The Biological Bulletin
- 786 198:203-212.
- 787 Webster D, Rahman S, Dasi L (2001) On the usefulness of bilateral comparison to tracking
- turbulent chemical odor plumes. Limnology and Oceanography 46:1048–1053.
- 789 Weissburg MJ, Zimmer-Faust RK (1994) Odor plumes and how blue crabs use them in
- 790 finding prey. Journal of Experimental Biology 197:349–375.

- 791 Wesson DW, Carey RM, Verhagen JV, Wachowiak M (2008) Rapid encoding and perception
- of novel odors in the rat. PLoS biology 6:e82.
- 793 Willis M, Avondet J (2005) Odor-modulated orientation in walking male cockroaches
- 794 Periplaneta americana, and the effects of odor plumes of different structure. Journal of
- respective experimental biology 208:721–735.

Figure Legends

797	Figure 1 Thermocouple implant, behavior arena and methods used for setup
798	standardization. (a) Schematic of rat's skull with thermocouple implant. (b) Schematic of
799	the behavior box with overhead camera. Compartments are indicated from C1 to C5. There
800	are dummy compartments between C1 and the wall, and C5 and the wall, to keep the odor
801	flow away from the walls. (c) Cross section of the behavior box and placement of
802	anemometer at grid lines for air flow measurement. (d) Odor plume visualization using plana
803	green laser light. (e) Olfactometer design in baseline IAA tracking experiments. (f)
804	Olfactometer design with background odor experiments. (g) Specified boundary regions for
805	defining trial outcome and strategy, color coded for each compartment. (h) Projected odor
806	path from each compartment used for calculation for deviation of trajectory from odor trail,
807	color coded from C1-C5.
808	Figure 2 Near Laminar Airflow in Behavior Box. (a) Heat map of the mean air flow
809	velocity in the box as measured by anemometer. (b) Heat map of the standard deviation of air
809 810	
	velocity in the box as measured by anemometer. (b) Heat map of the standard deviation of air
810	velocity in the box as measured by anemometer. (b) Heat map of the standard deviation of air flow velocity in the box. Air flow was very stable except near the walls. (c) Readout of
810 811	velocity in the box as measured by anemometer. (b) Heat map of the standard deviation of air flow velocity in the box. Air flow was very stable except near the walls. (c) Readout of Isoamyl acetate detection in the box using a photo ionization detector (PID) for the 5 central
810 811 812	velocity in the box as measured by anemometer. (b) Heat map of the standard deviation of air flow velocity in the box. Air flow was very stable except near the walls. (c) Readout of Isoamyl acetate detection in the box using a photo ionization detector (PID) for the 5 central compartments. White regions represent IAA presence. (d) Learning curve for correct odor
810 811 812 813	velocity in the box as measured by anemometer. (b) Heat map of the standard deviation of air flow velocity in the box. Air flow was very stable except near the walls. (c) Readout of Isoamyl acetate detection in the box using a photo ionization detector (PID) for the 5 central compartments. White regions represent IAA presence. (d) Learning curve for correct odor source location for all five rats. Chance accuracy level is 20% and criterion level for accuracy
810 811 812 813 814	velocity in the box as measured by anemometer. (b) Heat map of the standard deviation of air flow velocity in the box. Air flow was very stable except near the walls. (c) Readout of Isoamyl acetate detection in the box using a photo ionization detector (PID) for the 5 central compartments. White regions represent IAA presence. (d) Learning curve for correct odor source location for all five rats. Chance accuracy level is 20% and criterion level for accuracy is 80%. (e-f) Different tracking strategies based on trajectory of odor source location. Panel
810 811 812 813 814 815	velocity in the box as measured by anemometer. (b) Heat map of the standard deviation of air flow velocity in the box. Air flow was very stable except near the walls. (c) Readout of Isoamyl acetate detection in the box using a photo ionization detector (PID) for the 5 central compartments. White regions represent IAA presence. (d) Learning curve for correct odor source location for all five rats. Chance accuracy level is 20% and criterion level for accuracy is 80%. (e-f) Different tracking strategies based on trajectory of odor source location. Panel (e) is a direct trial while panel (f) represent examples of serial (left) or lateral scan (right) to

319	odor compartment. (g) Cumulative distribution of direct and serial trials as a function of trial
320	number, pooled across all baseline days and all rats.
321	Figure 3 Odor port vs. first compartment choice distributions. Panels (a-e) represent
322	data from 5 rats. Scatter plots show first entry against odor compartment, for each trial. Blue
323	dots indicate direct trials, and these are on the diagonals. Red dots represent scan trials. Data
324	is pooled for 10 days. Vertical histograms show distribution of first compartment entry.
325	These show a preference for a subset of compartments. Horizontal histograms below the
326	scatter plot are distribution of odor delivery compartments. As expected, these are flat
327	distributions. Right column shows histograms of average bin counts along diagonals, with
328	zero bin showing diagonal line, \pm 1 bins showing bins adjacent to diagonal, and so on. The
329	central bin is much larger than the others, in all cases. The ± 1 bins are larger than the other
330	off-diagonal bins in some cases.
331	Figure 4 Baseline measures of tracking strategies of trained rats. Data shown for days
331 332	Figure 4 Baseline measures of tracking strategies of trained rats. Data shown for days when accuracy was consistently higher than 80%. (a) Fraction of Direct trials for each rat. (b)
332	when accuracy was consistently higher than 80%. (a) Fraction of Direct trials for each rat. (b
332 333	when accuracy was consistently higher than 80%. (a) Fraction of Direct trials for each rat. (b) Percentage of correct Serial trials out of total number of Serial trials. (c) Average speeds of
332 333 334	when accuracy was consistently higher than 80%. (a) Fraction of Direct trials for each rat. (b) Percentage of correct Serial trials out of total number of Serial trials. (c) Average speeds of all rats across days for Direct (D, blue) and Serial (S, red) trials in the forward (F, solid lines)
332 333 334 335	when accuracy was consistently higher than 80%. (a) Fraction of Direct trials for each rat. (b) Percentage of correct Serial trials out of total number of Serial trials. (c) Average speeds of all rats across days for Direct (D, blue) and Serial (S, red) trials in the forward (F, solid lines) and reverse (R, dashed lines) direction. (d) Pooled data across all rats for all days. Forward
332 333 334 335 336	when accuracy was consistently higher than 80%. (a) Fraction of Direct trials for each rat. (b) Percentage of correct Serial trials out of total number of Serial trials. (c) Average speeds of all rats across days for Direct (D, blue) and Serial (S, red) trials in the forward (F, solid lines) and reverse (R, dashed lines) direction. (d) Pooled data across all rats for all days. Forward speeds (FD, FS) are significantly different from each other and from return speeds (RD, RS).
332 333 334 335 336 337	when accuracy was consistently higher than 80%. (a) Fraction of Direct trials for each rat. (b) Percentage of correct Serial trials out of total number of Serial trials. (c) Average speeds of all rats across days for Direct (D, blue) and Serial (S, red) trials in the forward (F, solid lines) and reverse (R, dashed lines) direction. (d) Pooled data across all rats for all days. Forward speeds (FD, FS) are significantly different from each other and from return speeds (RD, RS). No significant difference found between return speeds (*p =0, KW-Tukey HSD test. (e) Root
332 333 334 335 336 337	when accuracy was consistently higher than 80%. (a) Fraction of Direct trials for each rat. (b) Percentage of correct Serial trials out of total number of Serial trials. (c) Average speeds of all rats across days for Direct (D, blue) and Serial (S, red) trials in the forward (F, solid lines) and reverse (R, dashed lines) direction. (d) Pooled data across all rats for all days. Forward speeds (FD, FS) are significantly different from each other and from return speeds (RD, RS). No significant difference found between return speeds (*p =0, KW-Tukey HSD test. (e) Root mean square (RMS) deviation of rat trajectory from an extrapolated odor path for Direct (D,
3332 3333 3334 3335 3336 3337 3338	when accuracy was consistently higher than 80%. (a) Fraction of Direct trials for each rat. (b) Percentage of correct Serial trials out of total number of Serial trials. (c) Average speeds of all rats across days for Direct (D, blue) and Serial (S, red) trials in the forward (F, solid lines) and reverse (R, dashed lines) direction. (d) Pooled data across all rats for all days. Forward speeds (FD, FS) are significantly different from each other and from return speeds (RD, RS). No significant difference found between return speeds (*p =0, KW-Tukey HSD test. (e) Root mean square (RMS) deviation of rat trajectory from an extrapolated odor path for Direct (D, blue) and serial (S, red) trials. Solid lines represent forward direction (F) and dashed lines

843	time is significantly different for the two classified groups (KW-1 ukey HSD test, **p < 10 ",
844	panel (h)). Number of Direct trials, Nd, = 1851; Number of Serial trials, Ns, =2150. Legend 1
845	for panels (a-b). All error bars for panels (c, e, g) are in s.e.m. Panels (d, f, h) are box
846	whisker plots, representing the median (gray line), 25th percentile (bottom edge of box), 75th
847	percentile (top edge of box), most extreme data points (whiskers) and outliers marked
848	individually (gray crosses).
849	Figure 5 Instantaneous deviation of trajectory from odor path for each rat (panels a -
850	e). Deviation plotted for forward tracks only. Left column panels are deviations for direct
851	trials for one day. Deviation values are plotted as color scale (cm). Central and right columns
852	show examples of tracks for direct and serial trials respectively, overlaid on observed odor
853	plumes from Figure 2c. Tracks are color coded for each compartment. C1 - blue, C2 - red, C3
854	- pink, C4 - black and C5 - green Dashed lines represent boundaries of the box and the
855	compartments. HC = Holding Chamber; C1 to C5 are compartment numbers 1 to 5.
856	Figure 6 Rats sniff actively when going forward towards odor compartment. (a) Scatter
857	of sniff rate in forward path vs. return path averaged over entire dataset, all rats. Line is for
858	equal rates. Forward rate is almost always faster than return. (b) Sniff rate for direct and
859	serial trials is the same. Each point is mean of rate in serial trials vs. direct trials for a given
860	rat on a given day. Line is for equal rates. (c) Average sniff rate plotted against average
861	running speeds. Blue dots are forward direction and red dots are return. These form distinct
862	clusters. Forward sniff is faster, and run is slower, than return.
863	Figure 7: Instantaneous speed for direct trials plotted for each rat (panel a to panel e).
864	Left column panels are the speeds plotted for forward direction. Right column panels show
865	speeds in reverse direction. The color bars show the values of the speeds (in cm/s). X - axis is

867	represent boundaries of the box and the compartments. HC = Holding Chamber; C1 to C5 are
868	compartment numbers 1 to 5. The plots show multiple trials for a single day.
869	Figure 8: Instantaneous speed for serial trials plotted for each rat (panel a to panel e).
870	Left column panels are the speeds plotted for forward direction. Right column panels show
871	speeds in reverse direction. The color bars show the values of the speeds (in cm/s). X - axis is
872	the breadth of the box (in cm) and Y - axis is length of the box (in cm). Dashed lines
873	represent boundaries of the box and the compartments. HC = Holding Chamber; C1 to C5 are
874	compartment numbers 1 to 5. The plots show multiple trials for a single day.
875	Figure 9 Serial and Direct tracks diverge early after holding chamber. Tracks till first
876	entry shown for different compartments (a, e -C1; b, d, f -C2; c -C5) in direct (blue) and
877	serial (red) trials. Panels (a - c) shows non-overlapping tracks, while panels (d - f) shows
878	overlapping tracks for both direct and serial trials. First entries in direct trials are to the
879	correct odor compartment, while first entries in the serial trials are to the incorrect
880	compartment. Each panel shows tracks from a single session of an example rat as indicated in
881	the plot. (g) Deviation from odor plume (cm) as a function of distance from first entered
882	compartment (cm) averaged over all rats, shown for both direct (blue) and serial (red) trials.
883	(h) Example data from 2 rats showing deviation from odor plume in the initial 20 cm from
884	holding chamber. Rat B shows divergence of deviation for direct and serial trials after the 70
885	cm mark, where as all other rats show divergence from the beginning of the holding chamber
886	(100 cm). (i) Instantaneous speed averaged over all rats for every 1 cm towards first
887	compartment entered. Higher speed at 110 cm indicates turning of the animals from water
888	port. At approximately 70 cm, the direct and serial speeds begin to diverge from each other.

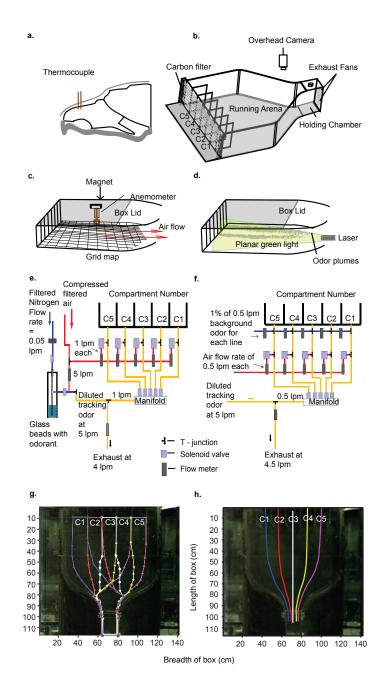
Figure 10 Rats rapidly learn to track novel odors. In panels (a-d, e, g, i), the white region
represents baseline (IAA) odor delivery; gray region represents Cineole, and red represents
Limonene (a) Total tracking accuracy. There is a major drop on introduction of cineole, a
smaller one for limonene. (b) Success rate in direct trials. There is a drop only in the first few
days with cineole. (c) Similar plot as (b) for serial trials. There is a big drop at the start of
cineole. (d) Fraction of trials using direct tracking for all rats. This drops towards chance
during the initial few days with cineole. (e) Average RMS deviation across all days for all
rats. There is remarkably little increase for forward direct trials. (f) Whisker box plot of RMS
deviation in forward direction for direct trials. Data is pooled for all rats. Nd (IAA) = 1851,
Nd (Cineole) = 921, Nd (Limonene) = 724. RMS values of days for Cineole and Limonene
are significantly different from IAA but not from each other (** $p < 10^{-10}$, KW-Tukey HSD
test). Gray line is the median. Lower and upper edges of the box represent 25th and 75th
percentile. Whiskers represent the extreme data points and gray crosses are the outliers. (g)
Mean forward and return speeds for direct (blue) and serial (red) trials for all rats in the
forward (solid lines) and return (dashed lines) direction. (h) Whisker bar plot of the average
mean speed for direct trials combined for days with IAA, Cineole and Limonene as tracking
odor. All speeds are significantly different from each other (** $p < 10^{-10}$, KW-Tukey HSD
test). Note that the speed distributions are positively skewed so the medians in the whisker
plots are higher than the means from panel g. (i) Total trial time averaged for all rats for
direct (blue) and serial (red) trials. (j) Whisker box plot for total trial times in direct tracking
for IAA, Cineole and Limonene days. Novel odors were significantly different from IAA, but
not from each other (** p < 10^{-25} , KW-Tukey HSD test). Error bars on all line plots are s.e.m.
values.
Figure 11 Nostril stitch does not affect accuracy. Gray shaded area represents the day of
unilateral stitch (a) Percentage of correct Direct trials out of total number of Direct trials (no

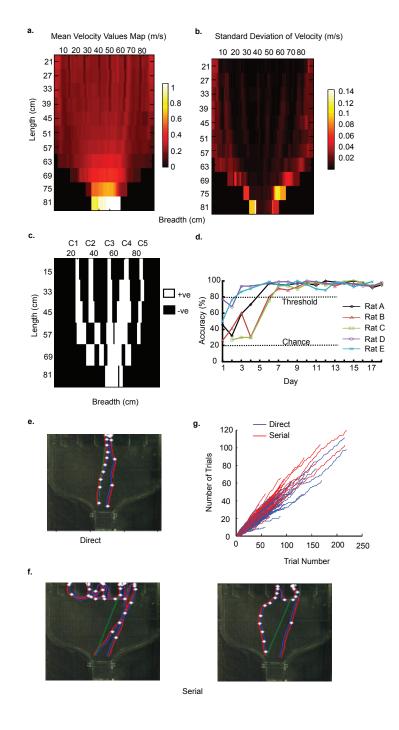
915	effect on accuracy, p > 0.05, Student's <i>t</i> - test). (b) Percentage of correct Serial trials out of
916	total number of Serial trials. (c) Fraction Direct trials. (d) Averaged RMS deviation pooled
917	for all rats for Direct (blue) and Serial (red) trials in forward (solid lines) and reverse (dashed
918	lines) direction. No significant differences were observed for RMS values (data not shown).
919	(e) Total trial time for all rats for Direct trials (blue) and Serial (red) trials. (f) Total time for
920	Direct trials pooled for all rats for 3 groups - Pre nostril stitch (Pre stitch, N = 425), Nostril
921	stitch (stitch, $N=92$), and post nostril stitch (post stitch, $N=243$). Total trial time for stitch
922	days are significantly higher than pre and post stitch days (** $p < 10^{-10}$, KW-Tukey HSD test)
923	(g) Mean forward and return speeds for all rats. (h) Mean speeds for direct trials in forward
924	direction. Stitch day speeds were significantly lower than pre and post stitch days (** $p < 10^{-7}$
925	KW-Tukey HSD test). Error bars on all line plots are s.e.m.
926	Figure 12 Background odor identity transiently affects accuracy of odor localization.
927	Foreground tracking odor is Limonene (0.5 %). Control (air background) is represented in
928	white. Rats take 1-2 days to stabilize to the reduced tracking odor concentrations. Linalool
929	background is gray shaded, Menthone is red shaded and IAA is green shaded. (a) Total
930	accuracy of all rats with background odors. There is a small drop for menthone, and a large
931	drop for IAA. (b) Fraction of direct trials for all rats. (c) Accuracy of direct (d) and serial
932	trials for all rats with different background odors. There is a particularly large dip for IAA.
933	(e) Average root mean square (RMS) deviation of all rats for direct and serial trials in
934	forward and return direction. (f) Averaged RMS deviation in direct trials during forward
935	tracking. Data pooled for all rats and trials. RMS deviation with air (Nd = 524) was
936	significantly different from days with Linalool (Nd = 295), but not from days with Menthone
937	(Nd = 241) as background (** p < 10^{-3} , KW-Tukey HSD test). RMS deviations for days with
938	IAA (Nd = 540) did not differ from air (Nd = 211, KW -Tukey HSD test). (g) Mean forward
939	and return speeds for direct and serial trials for different background odors. (h) Averaged

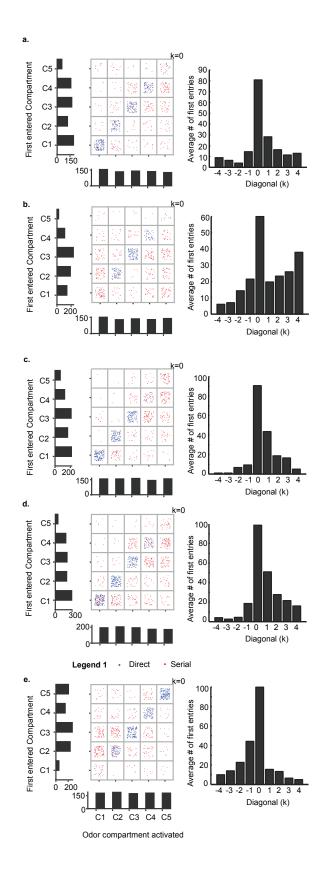
940	speeds for all direct trials during forward tracking with Linalool, Menthone and IAA as
941	background odors. Speeds for both Linalool and Menthone were significantly lower than
942	baseline (**p <10 ⁻⁸ , KW-Tukey HSD test). Speed for IAA (all days pooled) and air as
943	background were not significantly different. (i) Total trial time taken for different background
944	odors in direct and serial trials. (j) Average trial time for direct trials pooled across all days
945	for Air/ Linalool/ Menthone and Air/ IAA as background. Air background trial time is lower
946	than Linalool (* $p = 0.03$, KW - Tukey HSD test). Menthone as background did not affect trial
947	time. Average trial time pooled for days with IAA as background was not significantly
948	different than with background air (5% significance, KW-Tukey HSD test). Error bars on all
949	panels represent s.e.m values.
950	Figure 13 Increased Turbulence does not affect tracking accuracy. (a) Image of box
951	showing turbulent and (b) laminar flows, using smoke plumes illuminated by a laser light
952	sheet with the source near the holding chamber. Panels c-k : Gray shaded areas indicate days
953	when turbulence was introduced. (c) Accuracy of Direct trials and (d) Serial trials. (e)
954	Fraction of Direct Trials out of total trials. (f) Averaged root mean square (RMS) deviation
955	for all rats. (g) Whisker bar plot of average speed for direct trials in forward direction for
956	days with and without turbulence (Nd Laminar = 325, Nd Turbulence = 522). The RMS
957	values are significantly different from each other (** $p < 10^{-3}$, KW-Tukey HSD test). (h)
958	Forward and return speeds for direct and serial trials averaged across all rats. (i) Whisker bar
959	plot of mean speeds for days with near laminar and increased turbulence. Speed was
960	significantly lower for turbulent days (** $p < 10^{-14}$, KW-Tukey HSD test). (j) Trial time
961	averaged across all rats for direct and serial trials (k) Whisker bar plot of average trial time
962	for direct trials during near laminar and turbulent air flow. Trial time values are significantly
963	different from each other (** $p = 10^{-3}$, KW-Tukey HSD test). Error bars for all line plots
964	represent the s.e.m values.

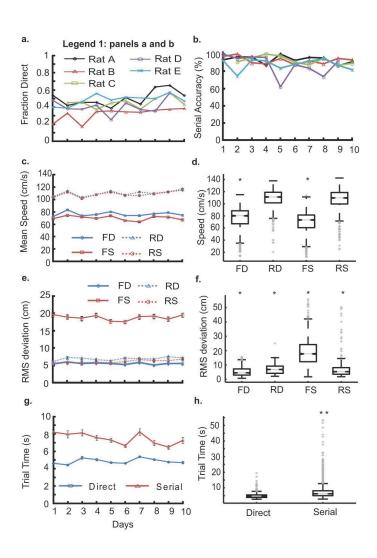
Figure 14 Trajectory changes are not triggered by odor sampling. Y axis shows average
displacement per frame since last sniff for forward track. X axis is time (msec) since last
sniff. Each data point is a successive frame. For each plot, black and blue represents example
data from different days. Star markers with dashed lines show control (see methods), while
circle markers represent post sniff (see methods) displacement values. Plots (a) and (b) shows
baseline tracking data for Rat A and D respectively. Plot (c) shows pre-stitch baseline for Rat
D while plot (d) shows (Limonene + IAA background) data for Rat D. The control and sniff
related displacements were not found to be significantly different from each other in all cases
(Z test, Bonferoni correction, at 0.001 significance level).
Figure 15 Run-and-scan behavior is usually faster than casting. Color maps of time
difference between casting and run-and-scan. X axis shows the distance to the source
(meters) and Y axis shows the number of possible targets. Casting would be preferable for
time difference less than 0 (blue shaded bins) while run-and-scan would be preferable for
time difference greater than 0 (red shaded bins). The black line indicates the parameters for
which they are equal. (a) Model 1, where rats find the correct adjacent compartment on the
second try. (b) Model 2, where there is no special advantage in finding odors in the adjacent
compartment.
Figure 16 Fraction Direct performance (a) Accuracy of direct trials over 10 days of
• • • • • • • • • • • • • • • • • • • •
baseline training for all 5 rats (Legend 1). (b - f) Data for all experiment subsets, i.e.
(Baseline - Novel odors (Cineole, Limonene) - Novel Background odor (Linalool,
Menthone) - Pre stitch - Stitch - Post stitch - IAA background - Turbulence) from 5 rats are
shown from panels (b) onwards. Each compartment is a color coded dashed line (Legend 2).
The plots show fraction from total entries into a given compartment when that compartment
was the odor port, i.e.

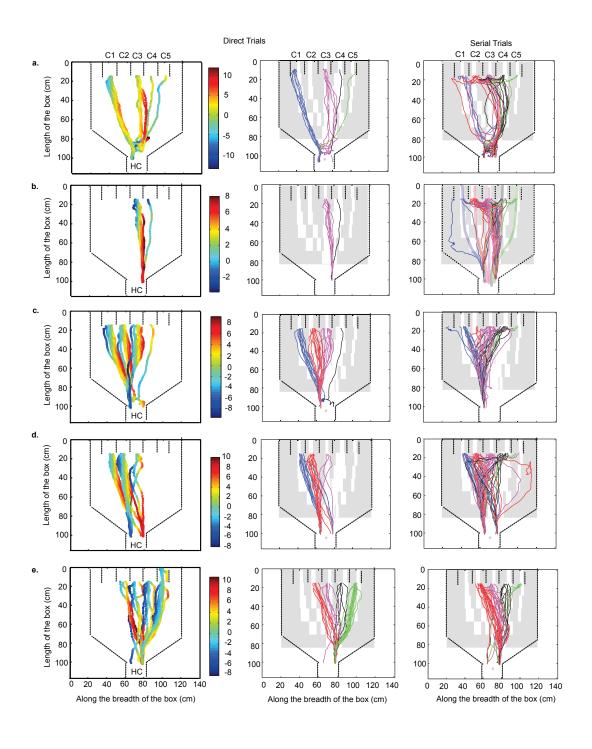
989	Fraction = Number of first entries in that compartment when odor was on / Total number of
990	first entries in that compartment
991	Figure 17 First compartment entries for different experimental modules. Panels a-e
992	represent data from 5 rats. Each column represents an experimental module. Column 1 is
993	days of novel odor (Cineole); Column 2 is days of tracking + novel background odor
994	(Limonene + Linalool); Column 3 is the day of uni-lateral nostril stitch and Column 4 is days
995	of tracking + familiar background odor (Limonene + IAA). Serial and direct trials are color
996	coded (Legend 1). Y-axis is the number of first entries in each compartment. X-axis is odor
997	compartment activated.
998	Movie 1: Laminar Air Flow – Top view of behavior box with laminar flow conditions.
999	Smoke plumes are released into the box from compartment number 5 and visualized using
1000	green laser light. Video recorded at 25 Hz.
1001	Movie 2: Direct Tracking – A rat implanted with thermocouple is tracking odor source by
1002	running directly towards it. Odor compartment number is 1. Video recorded at 60 Hz,
1003	playback at 30 Hz.
1004	Movie 3: Serial Tracking – A rat implanted with thermocouple is tracking odor source by
1005	lateral or serial scans. Odor compartment number is 3. Video recorded at 60 Hz, playback at
1006	30 Hz.
1007	Movie 4: Turbulent Air Flow – Top view of behavior box with turbulent flow conditions.
1008	Smoke plumes are released into the box from compartment number 4 and visualized using
009	green laser light. Video recorded at 25 Hz

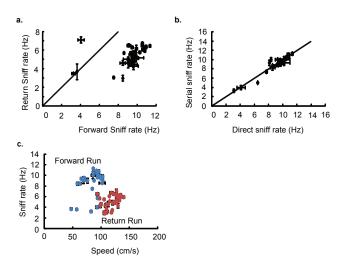


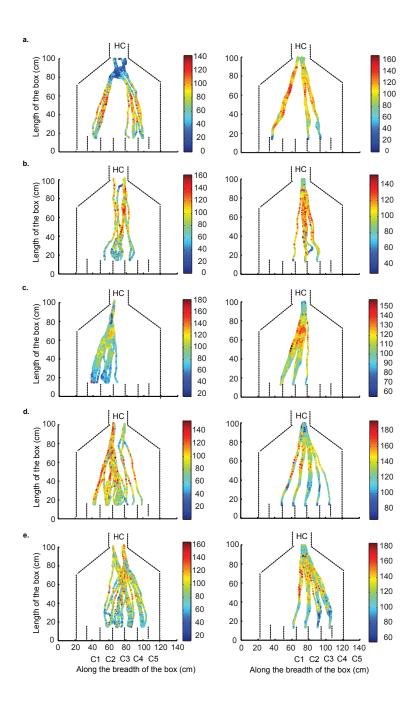


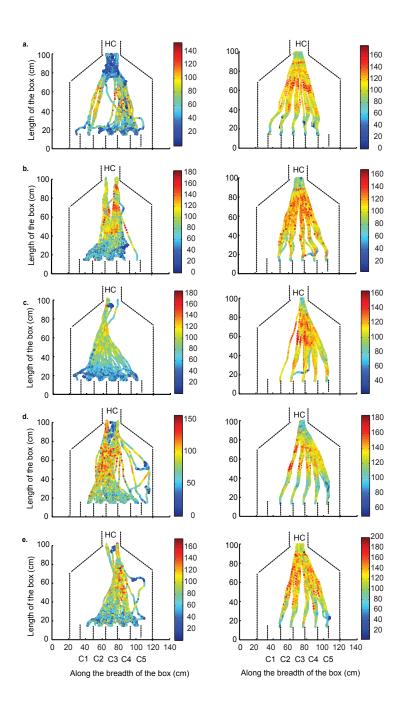


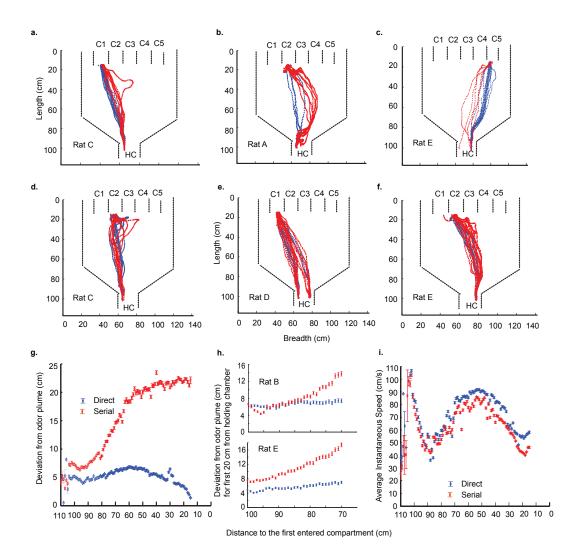


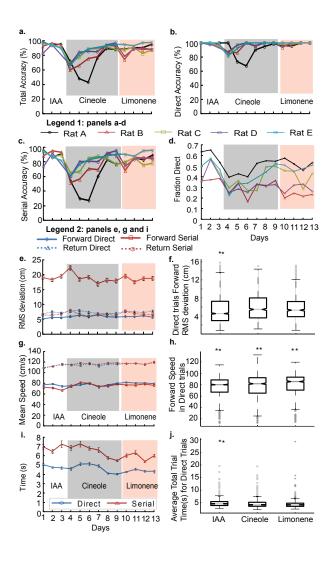


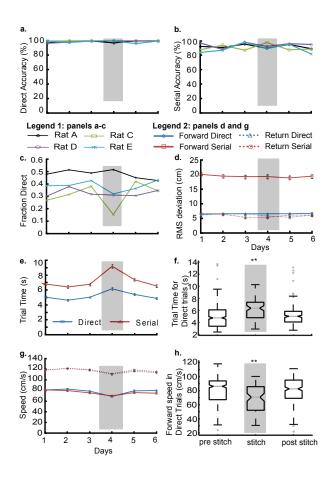


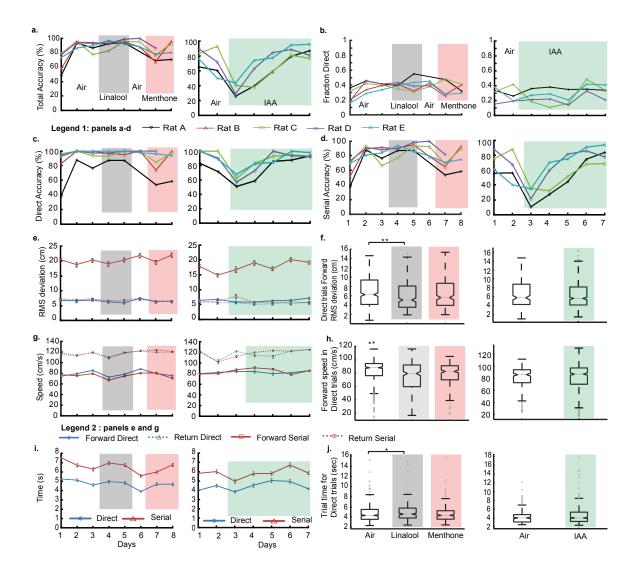


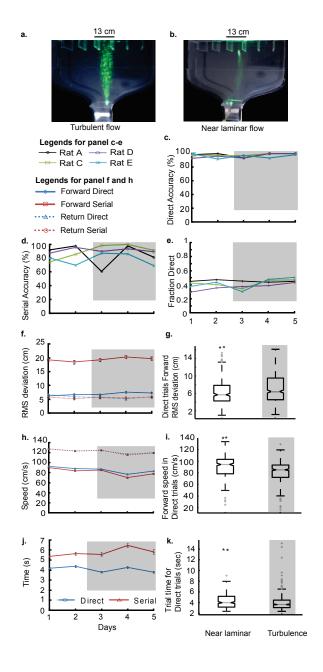


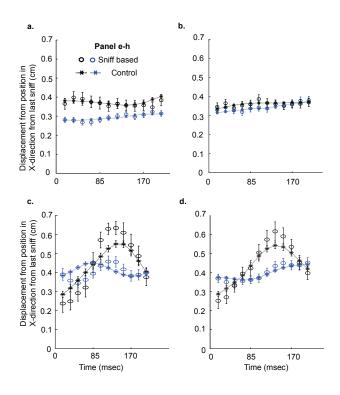


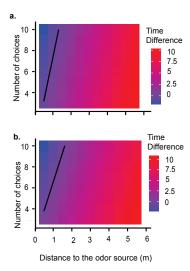


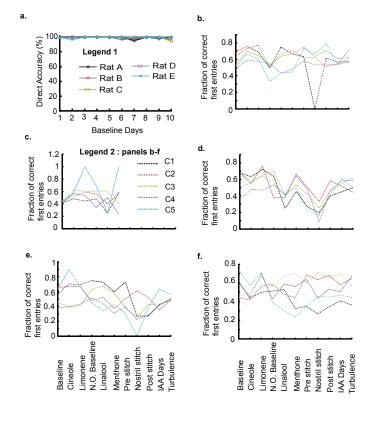


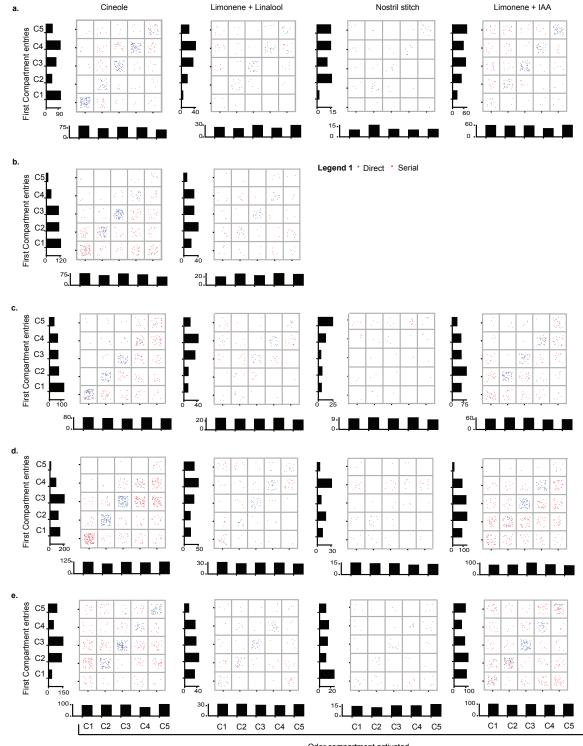












Odor compartment activated

